

ANISOTROPIC DAMAGE MODELLING OF COMPOSITE PLATES AND SHELLS

D. Benzerga^{1*}, A. Chouiter¹, A. Haddi² and A. Lavie²

¹University of Sciences and Technology of Oran, Mechanical Department, B.P. 1505, 31000 Oran, Algeria

²Univ. Artois, EA 4515, Laboratoire de Génie Civil et géo-Environnement (LGCgE), Béthune, F-62400, France

ABSTRACT

This paper deals with the analysis of geometrically nonlinear structures (plates, shells) of laminated composite materials by taking into account delamination phenomenon. We suggest a contribution to the modelling of the fibre reinforced composite materials damage in order to be able to predict the delamination of structures made of this type of material. The damage behaviour in large displacements was limited to the elastic domain with hypotheses of the moderate rotation theory including delamination phenomenon in the constitutive equations based on a damage model. This damage model was based on the use of damage mechanics considering three modes of interlaminar degradation which are associated with three modes of crack opening. Cracking has been described by a weakening of three stiffnesses acting in the three directions and damage variables are associated with the degradation of the stiffness matrix. Numerical simulations based on the finite element method were carried out predict the damage initiation and propagation of composite structures. The numerical results are compared with a number of similar results reported in the literature.

KEYWORDS: Modelling; Anisotropic damage; Delamination, Laminate composite

1.0 INTRODUCTION

For many years, a large number of damage models have been developed for multiple applications, from ductile materials to almost brittle behaviour. The mechanics of damage have changed considerably since Kachanov's first work (Kachanov, 1958). This formalism has shown its advantages in many applications. Without being exhaustive, we can cite (Chaboche, 1989), (Krajcinovic, 2010), and (Babu, 2010). Many models written in this framework are dedicated to the behaviour of composites. Different approaches can be distinguished: some study the microscopic scale and, by homogenization technique, deduce the behaviour on a larger scale (Rami, 2007-Blassiau, 2005), others are placed on the mesoscopic scale (that of the plies UD). In this latter group, several very satisfactory models of damage have been developed. We can cite the mesodel of Cachan developed by (Ladevèze et al, 2000) or the ONERA model (Laurin et al, 2007). Composite materials are inhomogeneous and generally anisotropic solids consisting of two or more materials of different natures. The model presented here is placed on a mesoscopic scale and is based on that developed by (Bui et al, 2017),

* Corresponding author e-mail: djeb_benz@yahoo.fr

(Babu, 2010), (Hinton et al, 2004) for composite materials. It is based on the theory of representation of tensor functions (Boehler, 1978), which are particularly suited to the modelling of anisotropic materials. It is thus desired to explore the capacities of these tools to reproduce the degradation of laminated composite shell subjected to stresses in large displacements. A formulation for anisotropic damage is established in the framework of the principle of strain equivalence. The damage variable is still related to the surface density of microcracks and microvoids and is represented by a second-order tensor. The coupling of the damage with the elasticity is written in tensor form. The evolution law is an extension of the classical law of isotropic damage. The damage tensor allows to link the actual stresses to their nominal quantities which are measurable externally (observable variables). The continuous description of the damage makes it possible to represent finely the initiation and propagation of the delamination in the stratified composite structures. The numerical results of delamination simulations are compared with those obtained from the literature give a good validation of the anisotropic model developed in this study.

2.0 LAMINATED COMPOSITE SHELL

The laminated shell is composed of a finite number of layers parallel to a reference surface Ω , chosen to coincide with the average surface of the first layer (Figure 1). Each layer has different physico-mechanical properties and different fiber orientations. The behavior of each layer is linearly elastic and anisotropic. The delamination is due to the interlaminar stresses which are exerted on weak interfaces. The material constituting each layer is assumed to be homogeneous and anisotropic, the anisotropy being symmetrical with respect to the reference surface Ω ($\theta^3 = 0$). Our material possesses three planes of symmetry, it is orthotropic (Kreja & Schmidt, 2005). The composite shell consists of orthotropic materials reinforced with fibers embedded in layers. Each layer is characterized by its orthotropy reference $\{\mathcal{G}^i\}$ such that the axis \mathcal{G}^1 is aligned with the direction of the fibers, while the axis \mathcal{G}^3 is normal to the average surface (Figure 1). In the system of axes $\{\mathcal{G}^i\}$, the components of the elasticity tensor relative to the reference axes of the fibers of the layer L are

$$\mathbf{C}_L = \tilde{C}_L^{abcd} \hat{e}_a \otimes \hat{e}_b \otimes \hat{e}_c \otimes \hat{e}_d \quad (1)$$

The tensor of the orthotropic material \tilde{C}_L can be written in matrix form $[\tilde{C}_L^{ijkl}] \in \mathbf{M}^{6 \times 6}$:

$$[\tilde{C}_L^{ijkl}] = \begin{bmatrix} \tilde{C}_L^{1111} & \tilde{C}_L^{1122} & \tilde{C}_L^{1133} & 0 & 0 & 0 \\ \tilde{C}_L^{1122} & \tilde{C}_L^{2222} & \tilde{C}_L^{2233} & 0 & 0 & 0 \\ \tilde{C}_L^{1133} & \tilde{C}_L^{2233} & \tilde{C}_L^{3333} & 0 & 0 & 0 \\ 0 & 0 & 0 & \tilde{C}_L^{2323} & 0 & 0 \\ 0 & 0 & 0 & 0 & \tilde{C}_L^{1313} & 0 \\ 0 & 0 & 0 & 0 & 0 & \tilde{C}_L^{1212} \end{bmatrix}_{6 \times 6} \quad (2)$$

Where the components \tilde{C}_L^{ijkl} take the following values (Barbero et al, 1990):

$$\begin{aligned}\tilde{C}_L^{1111} &= \frac{1 - \nu_{23}\nu_{32}}{E_2 E_3 \Delta}, \quad \tilde{C}_L^{1122} = \frac{\nu_{12} + \nu_{31}\nu_{23}}{E_2 E_3 \Delta} = \frac{\nu_{12} + \nu_{32}\nu_{13}}{E_1 E_3 \Delta} \\ \tilde{C}_L^{1133} &= \frac{\nu_{31} + \nu_{21}\nu_{32}}{E_2 E_3 \Delta} = \frac{\nu_{13} + \nu_{12}\nu_{13}}{E_1 E_3 \Delta}, \quad \tilde{C}_L^{2222} = \frac{1 - \nu_{13}\nu_{31}}{E_1 E_3 \Delta} \\ \tilde{C}_L^{2233} &= \frac{\nu_{32} + \nu_{12}\nu_{31}}{E_1 E_3 \Delta} = \frac{\nu_{23} + \nu_{21}\nu_{13}}{E_1 E_2 \Delta}, \quad \tilde{C}_L^{3333} = \frac{1 - \nu_{12}\nu_{21}}{E_1 E_2 \Delta}, \\ \tilde{C}_L^{2323} &= G_{23}, \quad \tilde{C}_L^{1313} = G_{13}, \quad \tilde{C}_L^{1212} = G_{12} \\ \text{avec } \Delta &= \frac{1 - \nu_{12}\nu_{21} - \nu_{23}\nu_{32} - \nu_{31}\nu_{13} - 2\nu_{21}\nu_{32}\nu_{13}}{E_1 E_2 E_3}.\end{aligned}\quad (3)$$

The elasticity tensor \mathbf{C}_L is determined by the 9 constants independent of the relations (3). The tensor \mathbf{C}_L must also be expressed in the coordinate system $\{g_i\}$ using following transformations (Figure 1)

$$\mathbf{C}_L = \tilde{C}_L^{abcd} \hat{e}_a \otimes \hat{e}_b \otimes \hat{e}_c \otimes \hat{e}_d = C_L^{ijkl} g_i \otimes g_j \otimes g_k \otimes g_l. \quad (4)$$

which leads to

$$C_L^{ijkl} = (g^i \cdot \hat{e}_a)(g^j \cdot \hat{e}_b)(g^k \cdot \hat{e}_c)(g^l \cdot \hat{e}_d) \tilde{C}_L^{abcd}. \quad (5)$$

The basic vectors in the coordinate systems \mathcal{G}^i and θ^i are linked by the following relation:

$$\hat{e}_a = \frac{\partial \theta^i}{\partial \mathcal{G}^a} g_i \quad (6)$$

For the layer L, the relation (5) becomes, then

$$C_L^{ijkl} = \frac{\partial \theta^i}{\partial \mathcal{G}^a} \frac{\partial \theta^j}{\partial \mathcal{G}^b} \frac{\partial \theta^k}{\partial \mathcal{G}^c} \frac{\partial \theta^l}{\partial \mathcal{G}^d} \tilde{C}_L^{abcd} \quad (7)$$

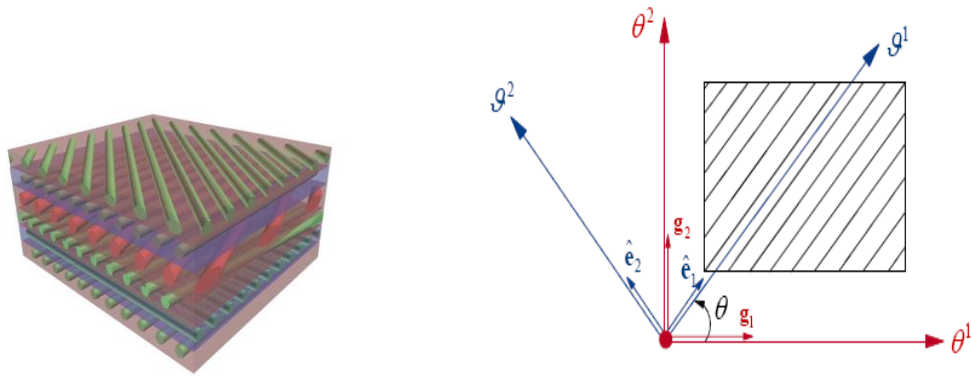


Figure 1. Main coordinates of a layer $\{\mathcal{G}^i\}$ and the curvilinear coordinates $\{\theta^i\}$.

The coordinate θ^3 always remains normal to the reference surface Ω and since $\theta^3 = \mathcal{G}^3$ we obtain

$$\mathbf{g}^3 \cdot \hat{\mathbf{e}}_a = 0, \quad \mathbf{g}^\alpha \cdot \hat{\mathbf{e}}_3 = 0, \quad \mathbf{g}^3 \cdot \hat{\mathbf{e}}_3 = 1. \quad (8)$$

when the vectors of the space base $\{\mathbf{g}_i\}$ are orthogonal, one obtains

$$\mathbf{g}^1 \cdot \hat{\mathbf{e}}_1 = \frac{\cos\theta}{\sqrt{g_{11}}}, \quad \mathbf{g}^2 \cdot \hat{\mathbf{e}}_1 = \frac{\sin\theta}{\sqrt{g_{22}}}, \quad \mathbf{g}^1 \cdot \hat{\mathbf{e}}_2 = -\frac{\sin\theta}{\sqrt{g_{11}}}, \quad \mathbf{g}^2 \cdot \hat{\mathbf{e}}_2 = \frac{\cos\theta}{\sqrt{g_{22}}} \quad (9)$$

where $g_{\alpha\alpha}$ (no summation) are the components of the metric tensor and θ the angle indicating the orientation of the fibres (Figure 1).

For an orthotropic material we have $C_L^{\alpha\beta\gamma 3} = 0$ and $C_L^{\alpha 333} = 0$ (Merzouki et al, 2007), therefore

$$\begin{aligned} S^{\alpha\beta} &= C_L^{\alpha\beta\lambda\gamma} E_{\lambda\gamma} + C_L^{\alpha\beta 33} E_{33} \\ S^{\alpha 3} &= 2C_L^{\alpha 3\lambda 3} E_{\lambda 3} \\ S^{33} &= C_L^{\alpha\beta 33} E_{\alpha\beta} + C_L^{3333} E_{33}. \end{aligned} \quad (10)$$

Greek indices take the values 1 and 2.

The above relationships can be written in matrix form by defining the matrix $\{S^{ij}\} \in \mathbf{M}^{6 \times 1}$ and $\{E^{ij}\} \in \mathbf{M}^{6 \times 1}$.

Then,

$$\begin{Bmatrix} S^{11} \\ S^{22} \\ S^{33} \\ S^{23} \\ S^{13} \\ S^{12} \end{Bmatrix} = \begin{bmatrix} C_L^{1111} & C_L^{1122} & C_L^{1133} & 0 & 0 & C_L^{1112} \\ C_L^{1122} & C_L^{2222} & C_L^{2233} & 0 & 0 & C_L^{2212} \\ C_L^{1133} & C_L^{2233} & C_L^{3333} & 0 & 0 & C_L^{3312} \\ 0 & 0 & 0 & C_L^{2323} & C_L^{2313} & 0 \\ 0 & 0 & 0 & C_L^{2313} & C_L^{1313} & 0 \\ C_L^{1112} & C_L^{2212} & C_L^{3312} & 0 & 0 & C_L^{1212} \end{bmatrix} \begin{Bmatrix} E_{11} \\ E_{22} \\ E_{33} \\ 2E_{23} \\ 2E_{13} \\ 2E_{12} \end{Bmatrix}. \quad (11)$$

The matrix $[C_L^{ijkl}] \in \mathbf{M}^{6 \times 6}$ in the curvilinear coordinate system $\{\theta^i\}$ can also be determined using the base change matrix $[T]$, such that

$$[C_L^{ijkl}] = [T][\tilde{C}_L^{ijkl}][T] \quad (12)$$

where $[T] \in \mathbf{M}^{6 \times 6}$ is denoted by

$$[T] = \begin{bmatrix} (d_{11})^2 & (d_{12})^2 & 0 & 0 & 0 & 2d_{11}d_{12} \\ (d_{21})^2 & (d_{22})^2 & 0 & 0 & 0 & 2d_{21}d_{22} \\ 0 & 0 & 1 & 0 & 0 & 0 \\ 0 & 0 & 0 & d_{22} & d_{21} & 0 \\ 0 & 0 & 0 & d_{12} & d_{11} & 0 \\ d_{11}d_{21} & d_{12}d_{22} & 0 & 0 & 0 & d_{11}d_{22} + d_{21}d_{12} \end{bmatrix}_{6 \times 6} \quad (13)$$

and $d_{ij} = \mathbf{g}^i \cdot \hat{\mathbf{e}}_j$ (see relationships (8) and (9)).

3.0 ANISOTROPIC DAMAGE

The damage in composite materials is due to the heterogeneities that give rise to stress concentrations. This case occurs at the interface between the fibre and the matrix, where decohesions can appear. Anisotropy also causes stress concentrations, especially at the interface between adjacent plies of different orientations, causing delamination. It is difficult to define a typical scenario which would lead to the failure of laminated composite structures, as the mechanisms of damage are numerous and complex [Ladeveze & Lubineau, 2003]. However, the phenomenon of delamination remains one of the most important problems faced by laminated composite materials. The phenomenon of delamination constitutes a particular case of anisotropic damage. Taking into account that the geometric effect of cavities and cracks, we can introduce on each element of area, spotted by its normal \vec{n} , an area reduction $\varpi(\vec{n})$ and the state of damage is characterized by a tensor of second order which is expressed in its main coordinate system by

$$\varpi = \sum_{j=1}^3 \varpi_j \vec{n}_j \otimes \vec{n}_j \quad (14)$$

Where ϖ_j and \bar{n}_j are the principal values and the unit vectors of the principal directions (directions which coincide with the axes of the material) of the tensor respectively. Symmetric tensor of damage of second order are most commonly used because of their mathematical simplicity compared to the tensor of higher order. They can describe most of anisotropic damage. However, these tensors of second order cannot represent a complicated state of damage such as orthotropic damage. The second order damage tensor were often used in the development of theories of anisotropic damage (Bui et al, 2017- Bielski et al, 2006- Chandra et al, 2008- Rajhi et all, 2014). Damage variables used to link the effective stresses at their nominal quantities that are measurable externally (observable variables). The law taking into account the damage behaviour is then written

$$S(E) = \check{C}(\varpi) \cdot E \quad (15)$$

where $\check{C}(\varpi)$ is the Hooke elasticity tensor for damaged material.

For a general state of deformation and damage, the nominal stress tensor can be connected to the tensor of the effective stresses by the following linear transformation

$$S = M \cdot \check{S} \quad (16)$$

which M is an operator of damage (order tensor 4). Following the shape used for tensor M , it is clear that from equation (3), the stress tensor S is generally not symmetrical. For the symmetry of tensor S , (Bui et al, 2017) use an energy equivalence instead of deformation equivalence and propose the following expression

$$S = \varpi^{-\frac{1}{2}} \cdot \check{S} \cdot \varpi^{-\frac{1}{2}} \quad (17)$$

The fourth order tensor of the damaged material corresponding to equation (16) can be defined by

$$M = \varpi^{-\frac{1}{2}} \cdot \check{\otimes} \cdot \varpi^{-\frac{1}{2}} \quad (18)$$

Then the tensor is symmetric

$$M_{ijkl} = M_{klij} = M_{jikl} = M_{ijlk} \quad (19)$$

For a virgin material (not damaged), $\varpi = I$ which corresponds to the identity transformation ($S = \check{S}$). In the literature, one can find the damage tensor denoted by the variable D such that

$$\varpi = (\sqrt{I - D})^{-1} \quad (20)$$

Tensors ϖ et \mathbf{D} have the same principal axes and principal values are such that (Andrew et al, 2008)

$$\varpi_j = \frac{1}{\sqrt{1-D_j}}. \quad (21)$$

D_j can be interpreted as the ratio of the area reduction in the plane perpendicular to \vec{n}_j caused by the development of cracks (Ganczarski et al, 2007). D_j varies between 0 and 1 while ϖ varies between 1 (virgin material) and $+\infty$ (completely damaged material). ϖ is considered as an internal state variable which characterizes the anisotropy of distribution of the microcracks in the material.

To determine the relationship between the strain tensor and stresses three approaches are used: strain equivalence, stress equivalence and energy equivalence. Unlike the equity deformation and stress, energy equivalence induces the symmetry of the tensor of rigidity and flexibility. This approach recognizes that the elastic energy stored in the damaged material is the same as the elastic energy stored in the equivalent virgin material, where in the nominal quantities by the effective amounts is replaced (Rouabhi, 2004):

$$\frac{1}{2} \mathbf{S} : \mathbf{E} = \frac{1}{2} \tilde{\mathbf{S}} : \tilde{\mathbf{E}} \quad (22)$$

From relations (17) and (22) is easily obtained

$$\mathbf{E} = \varpi^2 \cdot \tilde{\mathbf{E}} \cdot \varpi^2 \quad (23)$$

The degradation can be considered as the average effect of any microcracks developed in the material (Marriage, 2003). In this context, it is assumed that the material obeys the general law of Hooke in the damaged state (Ghosh & Sinha, 2005), then we can write

$$\tilde{\mathbf{S}}(\tilde{\mathbf{E}}) = \mathbf{C} \cdot \tilde{\mathbf{E}}. \quad (24)$$

Combining equations (22) and (23) with equations (24) and (15), one obtain

$$\begin{aligned} \mathbf{S} &= \varpi^{-1} \otimes \varpi^{-1} \cdot \mathbf{C} : \mathbf{E} \\ &= \mathbf{M} \cdot \mathbf{C} \cdot \mathbf{M} : \mathbf{E} \end{aligned} \quad (25)$$

where ϖ^{-1} is expressed by (Rohwer, 2014)

$$\varpi^{-1} = \sum_{j=1}^3 \frac{1}{\varpi_j} \vec{n}_j \otimes \vec{n}_j \quad (26)$$

Taking into account the relation (21), equation (26) is written yet

$$\varpi^{-1} = \sum_{j=1}^3 \sqrt{(1-D_j)} \bar{n}_j \otimes \bar{n}_j \quad (27)$$

The fourth tensor of equation \mathbf{M} then becomes

$$M = \varpi^{-\frac{1}{2}} \cdot \bar{\otimes} \cdot \varpi^{-\frac{1}{2}} = \begin{bmatrix} (\varpi_1)^{-1} & 0 & 0 & 0 & 0 & 0 \\ 0 & (\varpi_2)^{-1} & 0 & 0 & 0 & 0 \\ 0 & 0 & (\varpi_3)^{-1} & 0 & 0 & 0 \\ 0 & 0 & 0 & (\varpi_2 \varpi_3)^{-\frac{1}{2}} & 0 & 0 \\ 0 & 0 & 0 & 0 & (\varpi_1 \varpi_3)^{-\frac{1}{2}} & 0 \\ 0 & 0 & 0 & 0 & 0 & (\varpi_1 \varpi_2)^{-\frac{1}{2}} \end{bmatrix} \quad (28)$$

with $\varpi^{-\frac{1}{2}} = \sum_{j=1}^3 \frac{1}{\sqrt{\omega_j}} \bar{n}_j \otimes \bar{n}_j$.

The coupling between the damages ϖ_j (ϖ_j variables representing the damage in the principal directions of the tensor) makes it possible to write the fourth order tensor \mathbf{M} in the following form:

$$M = \varpi^{-\frac{1}{2}} \cdot \bar{\otimes} \cdot \varpi^{-\frac{1}{2}} = \begin{bmatrix} (\varpi_{11})^{-1} & 0 & 0 & 0 & 0 & 0 \\ 0 & (\varpi_{22})^{-1} & 0 & 0 & 0 & 0 \\ 0 & 0 & (\varpi_{33})^{-1} & 0 & 0 & 0 \\ 0 & 0 & 0 & (\varpi_{23})^{-\frac{1}{2}} & 0 & 0 \\ 0 & 0 & 0 & 0 & (\varpi_{13})^{-\frac{1}{2}} & 0 \\ 0 & 0 & 0 & 0 & 0 & (\varpi_{12})^{-\frac{1}{2}} \end{bmatrix} \cdot \quad (29)$$

Considering the relation (27), the fourth order tensor \mathbf{M} of the relation (29) can be written as

$$\begin{Bmatrix} S^{11} \\ S^{22} \\ S^{33} \\ S^{23} \\ S^{13} \\ S^{12} \end{Bmatrix} = \begin{bmatrix} (1-D_1)\tilde{C}_L^{11} & (1-D_2)\tilde{C}_L^{12} & (1-D_3)\tilde{C}_L^{13} \\ (1-D_1)\tilde{C}_L^{12} & (1-D_2)\tilde{C}_L^{22} & (1-D_3)\tilde{C}_L^{23} \\ (1-D_1)\tilde{C}_L^{13} & (1-D_2)\tilde{C}_L^{23} & (1-D_3)\tilde{C}_L^{33} \\ 0 & 0 & 0 \\ 0 & 0 & 0 \\ 0 & 0 & 0 \end{bmatrix} \begin{Bmatrix} E_{11} \\ E_{22} \\ E_{33} \\ 2E_{23} \\ 2E_{13} \\ 2E_{12} \end{Bmatrix} \quad (32)$$

$$\begin{bmatrix} 0 & 0 & 0 \\ 0 & 0 & 0 \\ 0 & 0 & 0 \\ (1-D_{23})\tilde{C}_L^{44} & 0 & 0 \\ 0 & (1-D_{13})\tilde{C}_L^{55} & 0 \\ 0 & 0 & (1-D_{12})\tilde{C}_L^{66} \end{bmatrix}$$

4.0 DELAMINATION

The interface between two plies may break under local stress peel and / or shear S^{13} and S^{23} (Figure 2). It then creates an interlaminar fracture called delamination.

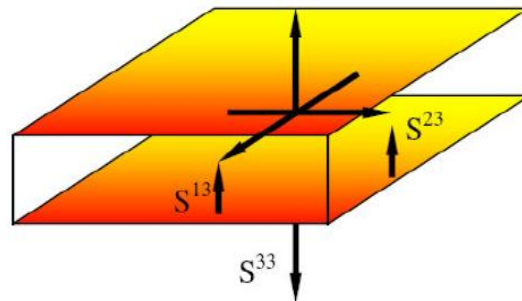


Figure 2. Interlaminar stresses responsible of delamination

Delamination only affects terms of shear and normal of the part above the plane strain field. Therefore the behaviour of law (10) for an orthotropic material, is written

$$\begin{aligned} S^{\alpha\beta} &= C_L^{\alpha\beta\lambda\gamma} E_{\lambda\gamma} + (1-D_{33})C_L^{\alpha\beta 33} E_{33} \\ S^{\alpha 3} &= 2(1-D_{\lambda 3})C_L^{\alpha 3\lambda 3} E_{\lambda 3} \\ S^{33} &= C_L^{\alpha\beta 33} E_{\alpha\beta} + (1-D_{33})C_L^{3333} E_{33}. \end{aligned} \quad (33)$$

Greek indices take the values 1 and 2.

The damages are closely coupled because the same microcracks are participating in the delamination phenomenon. Therefore, (Gupta et al, 2005) introduced an evolution law as:

$$\begin{cases} D_{33} = \omega(\widehat{Y}) \text{ if } D_{33} < 1 & D_{33} = 1 \text{ otherwise} \\ D_{13} = \gamma_1 \omega(\widehat{Y}) \text{ if } D_{13} < 1 \text{ and } D_{33} < 1 & D_{13} = 1 \text{ otherwise} \\ D_{23} = \gamma_2 \omega(\widehat{Y}) \text{ if } D_{23} < 1 \text{ and } D_{33} < 1 & D_{23} = 1 \text{ otherwise} \end{cases} \quad (34)$$

where $\omega(\widehat{Y}) = \left(\frac{n}{n+1} \frac{\langle \widehat{Y} - Y_0 \rangle}{Y_f - Y_0} \right)^n$

with $\widehat{Y} = \left[(Y_{33})^\rho + (\omega_1 Y_{13})^\rho + (\omega_2 Y_{23})^\rho \right]^{1/\rho}$ energy release rate equivalent [Gornet & Sinha, 2000]. ω_1 and ω_2 are coupling parameters between shear and transverse energy, and ρ another material parameter used to describe the shape of the fracture surface. In Fracture Mechanics ρ is determined by delamination tests in mixed mode [Aiello et al., 2003] and the rate of energy release in the three modes of delamination failures are defined as:

$$\begin{matrix} Y_{13} = \frac{1}{2} k_{13}^0 (u_{13})^2 & Y_{23} = \frac{1}{2} k_{23}^0 (u_{23})^2 & Y_{33} = \frac{1}{2} k_{33}^0 (u_{33})^2 \\ \text{mode III} & \text{mode II} & \text{mode I} \end{matrix} \quad (35)$$

k_{i3}^0 are the interface stiffness and $u_{i3}^0 (i=1,2,3)$ represent the relative displacements at the interface. We can observe that the more the interface is ‘strong’ and the more the coefficient n is important. Y_0 and Y_f are initiation and rupture threshold delamination (see Benzerga, et al, 2014).

5.0 APPLICATION EXAMPLES

In this section, numerical investigations are presented and our results are compared to analytical solutions found in literature in order to validate our model.

5.1 Composite plate (0/90)

The first plate is composed of two layers (0/90) cantilever subjected to a shearing force evenly distributed at its free end (Figure 3). This plate has 100 mm of length (L), 10 mm of width (b) and 3 mm of thickness (h). The mechanical properties of laminated composite are presented in Table 1.

Table 1. Mechanical characteristics of composite

Young’s modulus		Shear Modulus		Poisson coefficient
E_{11}	$E_{22}=E_{33}$	$G_{12}=G_{13}$	G_{23}	$\nu_{12}=\nu_{13}=\nu_{23}$
1.0×10^3	0.3×10^3	0.15×10^3	0.12×10^3	0.25
GPa	GPa	GPa	GPa	

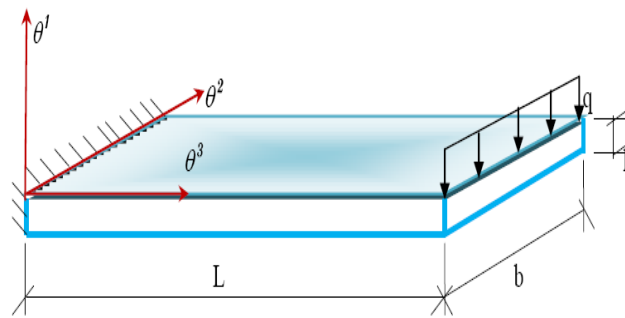


Figure 3. Composite plate (0/90) cantilevered

The second plate is composed of two layers (0/90) subjected to a uniform pressure (Figure 4). This plate has 228.6 mm of length (L), 38.1 mm of width (b) and 1.016 mm of thickness (h). The mechanical properties of laminated composite are presented in Table 2.

Table 2. Mechanical characteristics of composite

Young's modulus		Shear Modulus		Poisson coefficient
E_{11}	$E_{22}=E_{33}$	$G_{12}=G_{13}$	G_{23}	$\nu_{12}=\nu_{13}=\nu_{23}$
140 GPa	9.8 GPa	4.9 GPa	0.84 GPa	0.3

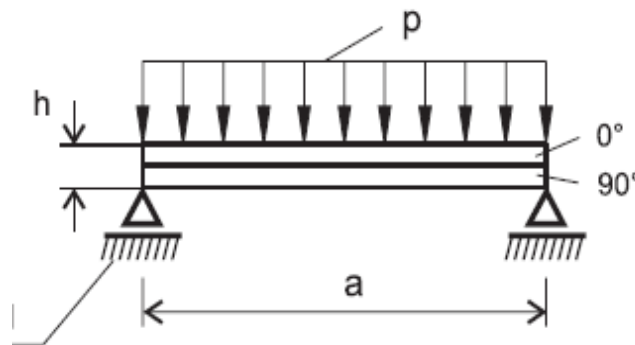
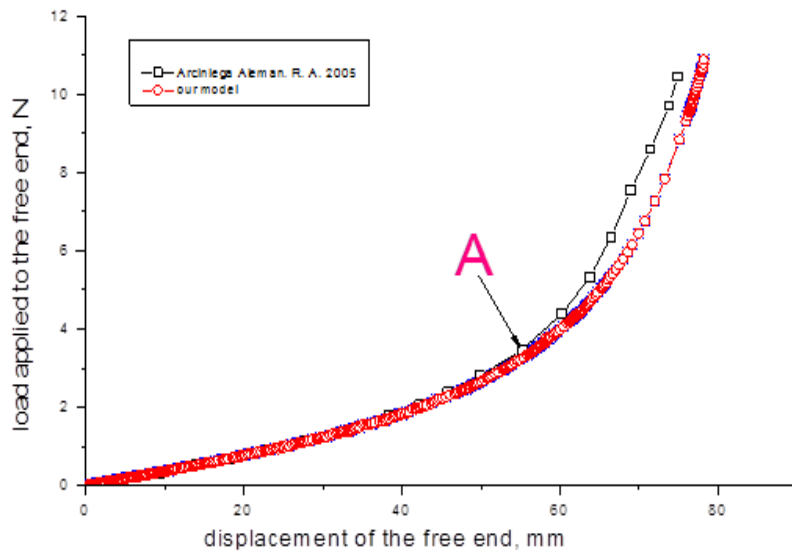
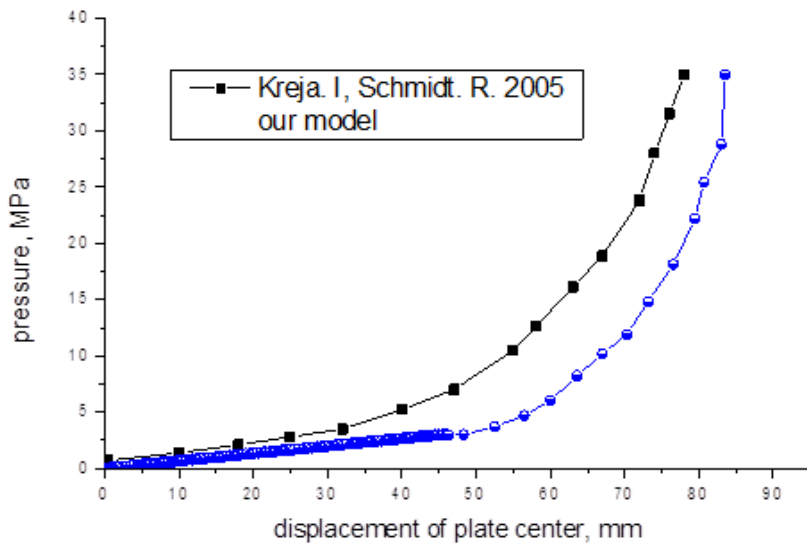


Figure 4. Composite Plate (0/90) under pressure

Figure 5 presents the evolution of the applied force or pressure versus displacement. This figure illustrates the comparison between the present study and analytical results from (Kreja & Schmidt, 2005) and (Arciniega, 2005). Analytical results correspond to the shell theory without taking into account the damage phenomenon. It should be noted that, from zero to A, the two curves have similar behaviour with an absence of any damage phenomena. From point A, the two curve diverge resulting from the damage initiation and propagation at the composite interface. However, the nature of applied load has an influence on the initiation of delamination. The results obtained show that for applied force the damage initiation starts at 60 mm of displacement (Figure 5a), whereas for applied pressure the damage starts at 10 mm of displacement (Figure 5b).



(a)



(b)

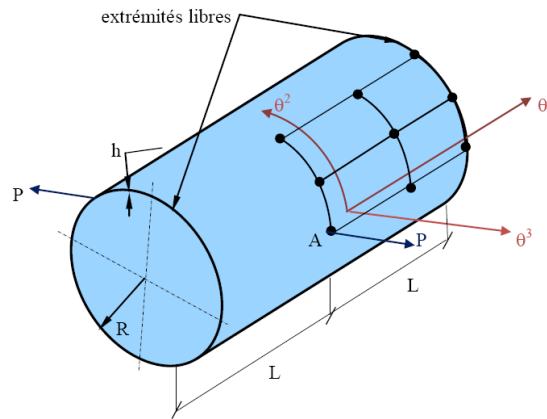
Figure 5. Displacement of the center of the plate (a) shearing force and (b) under pressure loading

5.2. Stretching of an open thin cylinder

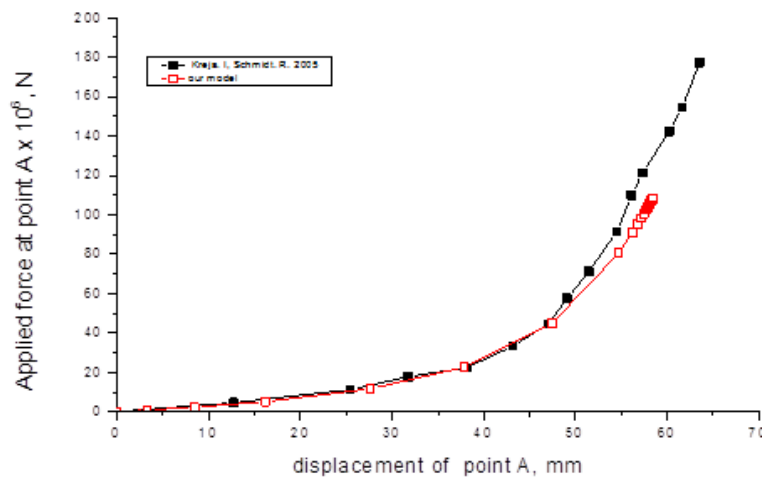
This example is the most requested test in the literature for the analysis of isotropic shells moderate rotations. Currently, composite variations of this test have been proposed. A laminate cylinder (0/90) of short length subjected to two opposing forces in its central section, both ends remain free (see Figure 6a). This cylinder has 131.445 mm of length (L), 125.8062 mm of radius (R) and 2.3876 mm of thickness (h). The cylinder is characterized by the geometrical data and the following mechanical properties (Table 3).

Table 3. Mechanical characteristics of cylinder

Young's modulus		Shear Modulus		Poisson coefficient
E_{11}	$E_{22}=E_{33}$	$G_{12}=G_{13}$	G_{23}	$\nu_{12}=\nu_{13}=\nu_{23}$
213.5 MPa	73.5 MPa	28 MPa	28 MPa	0.3125



(a) A laminate cylinder (0/90) subjected to two opposing forces in its central section



(b) Displacement curve of laminate cylinder center A

Figure 6. Behaviour cylinder (0/90) under two opposing forces in its central section

5.3 Laminated cylindrical panel secured at both ends subjected to a concentrated load in the middle.

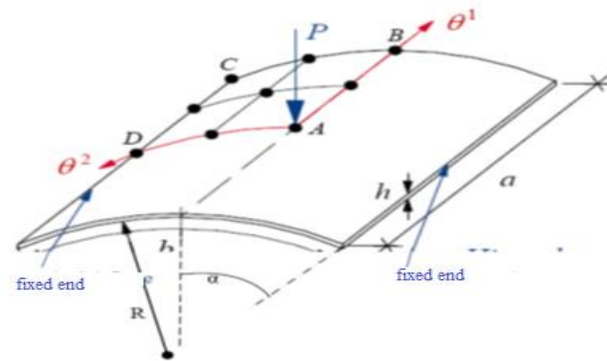
Figure 7 shows a cylindrical laminate panel (0/90/0/90) is submitted to concentrated force in its centre. The mechanical and geometrical properties are presented in Table 4 and 5.

Table 4. Mechanical characteristics of cylinder

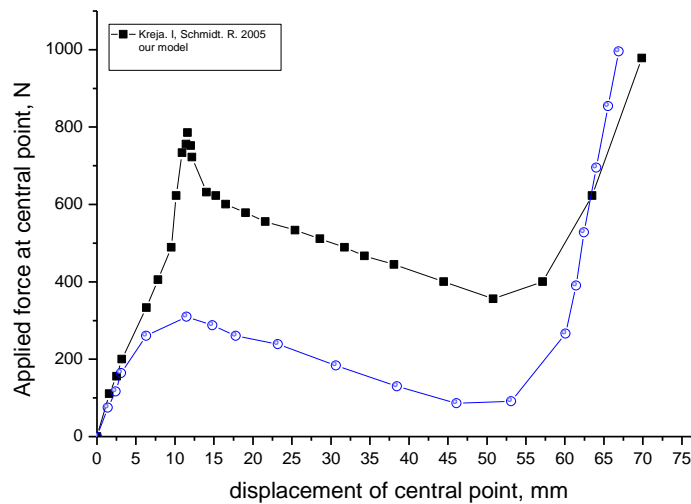
Young's modulus		Shear Modulus (MPa)		Poisson coefficient
E_{11}	$E_{22}=E_{33}$	$G_{12}=G_{13}$	G_{23}	$\nu_{12}=\nu_{13}=\nu_{23}$
143.22×10^3	34.44×10^3	17.76×10^3	17.76×10^3	0.313
MPa	GPa	MPa	MPa	

Table 5. Geometry of cylinder

Length	Radius	Angle	Thickness (mm)
L (mm)	R (mm)	α ($^\circ$)	h (mm)
139.7	304.8	0.5	1.016



(a) Laminated cylindrical panel submitted to concentrated force in its centre



(b) Displacement of laminated cylindrical panel center

Figure 7. Behaviour of laminated cylindrical panel subjected to a concentrated load at its centre.

Figure 7 shows the result of the central displacement of cylindrical panel according to the central load. It can be seen that the buckling load predicted by our approach is close to that obtained by (Kreja and Schmidt 2005). However, a difference appears in the post-buckling region when the delamination begins to appear.

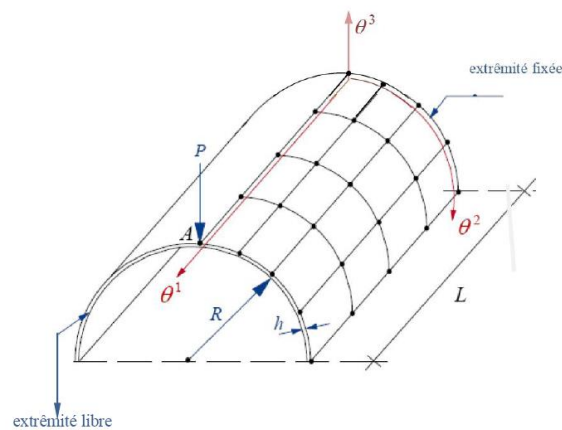
5.4. Semi-cylindrical shell

Figure 8 shows the laminated half-cylinder (0/90/0) subjected to a concentrated load applied to its free end. This cylinder has 304 mm of length (L), 101.6 mm of radius (R) and 3.3 of thickness (h). The material composite properties are presented in Table 6.

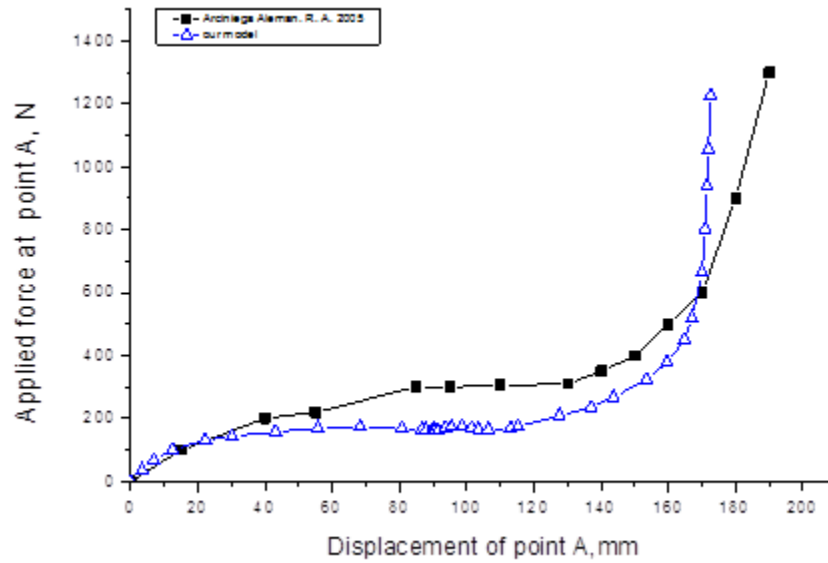
Table 6. Mechanical characteristics of cylinder

Young's modulus		Shear Modulus		Poisson coefficient
E_{11}	$E_{22}=E_{33}$	$G_{12}=G_{13}$	G_{23}	$\nu_{12}=\nu_{13}=\nu_{23}$
2068.5 MPa	517.125 MPa	795.6 MPa	198.89 MPa	0.3

Figure 8 shows the displacements of the point A compared to those of reference [Arciniega Aleman, 2005]. The results are quite close before the appearance of delamination phenomenon.



(a) Laminated half-cylinder subjected to force in its center



(b) Displacement of the centre A of laminated half-cylinder

Figure 8. Behaviour of the laminated half-cylinder submitted to load in its centre

6.0 CONCLUSIONS

An anisotropic damage model, based on the concept of continuum damage mechanics, was developed to simulate the delamination phenomenon in laminated composite shells composed of unidirectional plies subjected to large displacement. These composite structures have the enormous advantage of being able to adapt to any loading by orienting the fibers according to the direction of stresses. The behavior was limited to the elastic domain with the assumptions of the moderate rotational theory (MRT5) including the delamination phenomenon in the constitutive equations. Using the ansys programmable language, subroutine was developed and implemented in the main code. Different geometries have been used to validate the damage model presented in this study for predicting delamination initiation and propagation. The results of these first simulations, are in good agreement with the results obtained from the literature, indicate that the proposed model is able to describe the degradation modes in composite structures. They open the way to many perspectives. In the first stage, it is now necessary to compare the simulations on composite structures, whose stacking sequence is more complex. It is also desired to introduce into the developed model all the types of degradation to which a laminated shell could be confronted.

REFERENCES

- Andrew T. R., Richard, B., & Giles W. H. (2008). Post-buckled propagation model for compressive fatigue of impact damaged laminates. *International Journal of Solids and Structures*. 45, 4349–4361
- Arciniega, A. R. A. (2005). On a tensor-based finite element model for the analysis of shell structures. *Dessertation submitted to the Office of Graduate of Texas A & M University*, in partial fulfilment of requirements for degree of PhD.
- Babu, R.R., Benipal G. S., & Singh A. K. (2010) Constitutive model for bimodular elastic damage of concrete. *Latin American Journal of Solids and Structures*. 7(2).
- Barbero, E. J., Reddy, J. N., & Teply, J. L. (1990). General two-dimensional theory of laminated cylindrical shells. *American Institute of Aeronautics and Astronautics Journals*. 28 (3) 544–553.
- Benzerga, D., Haddi, A., Lavie, A. (2014). Delamination Model Using Damage Mechanics Applied to New Composite for Orthopaedic Use, *International Journal of Materials Engineering*, 4(3). 103–113.
- Bielski, J., Skrzypek, J. J., & Kuna-Ciskal, H. (2006). Implementation of a Model of Coupled Elastic-Plastic Unilateral Damage Material to Finite Element Code. *International Journal of Damage Mechanics, SAGE Publications*, 15 (1). 5–39.
- Blassiau, S. (2005). Modélisation des phénomènes microstructuraux au sein du composite unidirectionnel carbone/époxy et prédiction de durée de vie : contrôle et qualification de réservoirs bobinés. *Rapport de thèse*, Ecole des mines de Paris.
- Boehler, P. (1978). Lois de comportement anisotrope des milieux continus. *J Meca*, vol.17, pp 153 – 190.
- Bui, T.A., Wong, H., Deleruyelle, F., Xie, L.Z., & Tran, D.T. (2017). A thermodynamically consistent model accounting for viscoplastic creep and anisotropic damage in unsaturated rocks », *International Journal of Solids and Structures*, Volume 117, Pages 26-38.
- Chaboche, J. L. (1989). Continuum damage mechanics, parts II and I. *ASME J Appl Mech*, pp. 55-59 and 55-65.
- Chandra, V. S., & Ramesh, T. (2008). Analysis of multiple off-axis ply cracks in composite laminates. *International Journal of Solids and Structures*. Volume 45, Issue 16, 1 August, Pages 4574-4589

- Ganczarski, A., Barwacz, L., & Ganczarski, A. (2007). Low Cycle Fatigue Based on Unilateral Damage Evolution', *international journal of damage mechanics*, Vol 16, Issue 2.
- Ghosh, A., & Sinha, P.K. (2005). Initiation and propagation of damage in laminated composite shells due to low velocity impact. *Woodhead publishing Ltd*, U Crash, Vol. 10.
- Gornet, L., Leveque, D., & Perret, P. (2000). Modélisation, identification et simulations éléments finis des phénomènes de délaminage dans les structures composites stratifiées. *Mécanique and Industries / Mécanique et Industries*, EDP Sciences, Numéro Spécial Matériaux Composites. 1(3), 267-276.
- Gupta, A.K., Patel, B. P., & Nath, Y. (2015). Progressive damage of laminated cylindrical/conical panels under meridional compression. *European Journal of Mechanics - A/Solids*. 53, 329-341.
- Hinton, M.J., Kaddour, A.S., & Soden, P.D. (2004). Evaluation of failure prediction in composite laminates: background to 'part C' of the exercise. *Computer Science and Technology*. 64, 32 – 327.
- Kachanov, L. M. (1958). On the time to failure under creep conditions. *Izv AN SSSR, Otd tekhn.* 31,8-31.
- Krajcinovic, D. (2010). Continuum damage mechanics. *Applied Mechanics Review*. 37.
- Kreja, I., & Schmidt, R. (2006). Large rotations in first-order shear deformation FE analysis of laminated shells. *International Journal of Nonlinear Mechanics*, 41(1), 101-123
- Ladevèze, P., & Lubineau. G. (2003). On a damage mesomodel for laminates: micromechanics basis and improvement. *Mechanics of Materials*. 35(8), 763-775.
- Ladeveze, P., Allix, O., Deu, J-F., & Eveque, D. (2000). A mesomodel for localization and damage computation in laminates. *Computer Methods in Applied Mechanics and Engineering*. 183,105-122.
- Laurin F., CARRERE, N., & MAIRE, J-F. (2007). A multiscale progressive failure approach for composite laminates based on thermodynamical viscoelastic and damage models. *Composites: Part A*, 38,198-209.
- Mariage, J. F. (2003). Simulation numérique de l'endommagement ductile en forgeage de pièces massives. *Thèse de l'Université de Technologie de Troyes*.
- Merzouki,T., Chalal, H., & Meraghni, F. (2007). Identification of Orthotropic Material Behaviour Using the Error in Constitutive Equation. *Experimental Analysis of Nano and Engineering Materials and Structures Proceedings of the 13th*

International Conference on Experimental Mechanics, Alexandroupolis, Greece, July 1–6, 2007.

Rajhi, W., Saanouni, K., & Sidhom, H. (2014). Anisotropic ductile damage fully coupled with anisotropic plastic flow: Modeling, experimental validation, and application to metal forming simulation. *International Journal of Damage Mechanics*. 23(8).

Rami, H. A., Kilic, H., & Mulina, A. (2007). Nested nonlinear micromechanical and structural models for the analysis of thick –section composite materials and structures. *Computer Science and Technology*. 67, 1993 – 2004.

Rohwer, K. (2014). Predicting fiber composite damage and failure. *Journal of Composite Materials*. DOI: 10.1177/0021998314553885 ISSN 0021-9983.

Rouabhi, A. (2004). Comportement et fragmentation dynamique des matériaux quasi fragiles. *Thèse de l'Ecole Nationale Supérieure des Mines de Paris*.